Since January 2020 Elsevier has created a COVID-19 resource centre with free information in English and Mandarin on the novel coronavirus COVID-19. The COVID-19 resource centre is hosted on Elsevier Connect, the company's public news and information website.

Cell

Low-dose Ad26.COV2.S protection against SARS-CoV-2 challenge in rhesus macaques

Graphical abstract

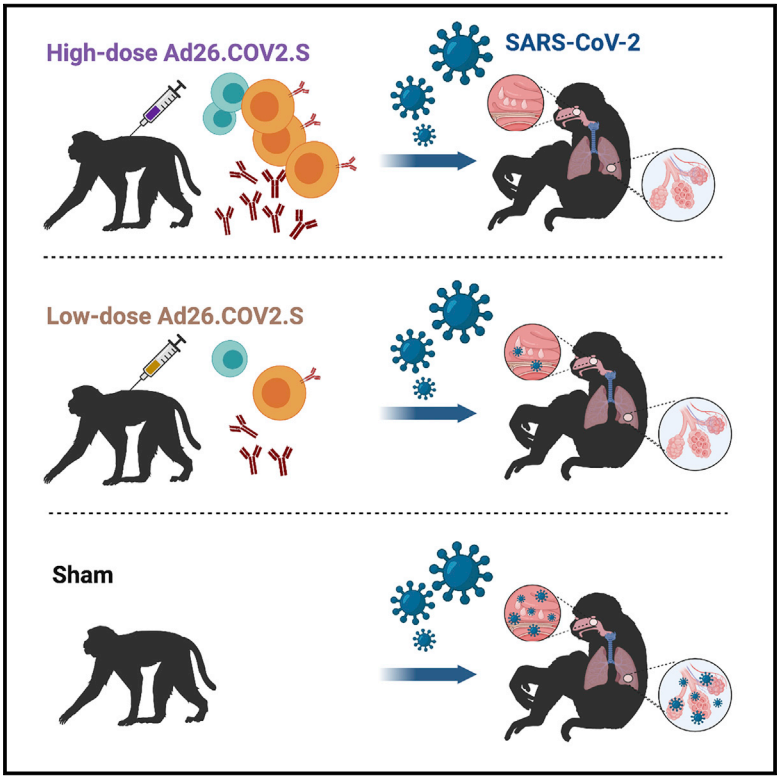

Authors

Xuan He, Abishek Chandrashekar, Roland Zahn, ..., Mark G. Lewis, Hanneke Schuitemaker, Dan H. Barouch

Correspondence

dbarouch@bidmc.harvard.edu

In brief

Evaluation of a reduced dosage of the single-shot Ad26.COV2.S reveals protection against SARS-CoV-2 challenge without enhancement of disease. A higher dosage may be needed for protection in the upper respiratory tract.

Highlights

- Low-dose single-shot Ad26 vaccine protects macaques against SARS-CoV-2 infection
- Higher vaccine dose may be required for protection in the upper respiratory tract
- Vaccine-induced memory B cells and antibodies correlate with protective efficacy

He et al., 2021, Cell *184*, 3467–3473
June 24, 2021
https://doi.org/10.1016/j.cell.2021.05.040

CellPress

Cell

CellPress

Article

Low-dose Ad26.COV2.S protection against SARS-CoV-2 challenge in rhesus macaques

Xuan He,[1,7] Abishek Chandrashekar,[1,7] Roland Zahn,[3,7] Frank Wegmann,[3,7] Jingyou Yu,[1,7] Noe B. Mercado,[1,7] Katherine McMahan,[1,7] Amanda J. Martinot,[2,7] Cesar Piedra-Mora,[2,7] Sidney Beecy,[2] Sarah Ducat,[2] Ronnie Chamanza,[3] Sietske Rosendahl Huber,[3] Marjolein van Heerden,[3] Leslie van der Fits,[3] Erica N. Borducchi,[1] Michelle Lifton,[1] Jinyan Liu,[1] Felix Nampanya,[1] Shivani Patel,[1] Lauren Peter,[1] Lisa H. Tostanoski,[1] Laurent Pessaint,[4] Alex Van Ry,[4] Brad Finneyfrock,[4] Jason Velasco,[4] Elyse Teow,[4] Renita Brown,[4] Anthony Cook,[4] Hanne Andersen,[4] Mark G. Lewis,[4] Hanneke Schuitemaker,[3] and Dan H. Barouch[1,5,6,8,*]

[1]Center for Virology and Vaccine Research, Beth Israel Deaconess Medical Center, Harvard Medical School, Boston, MA 02215, USA
[2]Tufts University Cummings School of Veterinary Medicine, North Grafton, MA 01536, USA
[3]Janssen Vaccines & Prevention BV, Leiden, the Netherlands
[4]Bioqual, Rockville, MD 20852, USA
[5]Ragon Institute of MGH, MIT, and Harvard, Cambridge, MA 02139, USA
[6]Massachusetts Consortium on Pathogen Readiness, Boston, MA 02215, USA
[7]These authors contributed equally
[8]Lead contact
*Correspondence: dbarouch@bidmc.harvard.edu
https://doi.org/10.1016/j.cell.2021.05.040

SUMMARY

We previously reported that a single immunization with an adenovirus serotype 26 (Ad26)-vector-based vaccine expressing an optimized SARS-CoV-2 spike (Ad26.COV2.S) protected rhesus macaques against SARS-CoV-2 challenge. To evaluate reduced doses of Ad26.COV2.S, 30 rhesus macaques were immunized once with 1×10^{11}, 5×10^{10}, 1.125×10^{10}, or 2×10^{9} viral particles (vp) Ad26.COV2.S or sham and were challenged with SARS-CoV-2. Vaccine doses as low as 2×10^{9} vp provided robust protection in bronchoalveolar lavage, whereas doses of 1.125×10^{10} vp were required for protection in nasal swabs. Activated memory B cells and binding or neutralizing antibody titers following vaccination correlated with protective efficacy. At suboptimal vaccine doses, viral breakthrough was observed but did not show enhancement of disease. These data demonstrate that a single immunization with relatively low dose of Ad26.COV2.S effectively protected against SARS-CoV-2 challenge in rhesus macaques, although a higher vaccine dose may be required for protection in the upper respiratory tract.

INTRODUCTION

Immune correlates of protection against SARS-CoV-2 have yet to be defined in humans. We recently reported that purified immunoglobulin G (IgG) from convalescent rhesus macaques protected naive animals against SARS-CoV-2 challenge in a dose-dependent fashion and that cellular immune responses may also contribute to protection (McMahan et al., 2021). We previously demonstrated that an adenovirus serotype 26 (Ad26) vector (Abbink et al., 2007) expressing a stabilized SARS-CoV-2 spike (Bos et al., 2020; Wrapp et al., 2020), termed Ad26.COV2.S, effectively protected rhesus macaques against SARS-CoV-2 infection and protected hamsters against severe SARS-CoV-2 disease (Mercado et al., 2020; Tostanoski et al., 2020). In these studies, vaccine-elicited binding and neutralizing antibodies (NAbs) correlated with protection (Mercado et al., 2020; Tostanoski et al., 2020). DNA vaccines, mRNA vaccines, ChAdOx1 vectors, and inactivated virus vaccines have also been reported to protect against SARS-CoV-2 challenge in macaques (Corbett et al., 2020; Gao et al., 2020; van Doremalen et al., 2020; Wang et al., 2020; Yu et al., 2020).

In multiple SARS-CoV-2 vaccine studies in non-human primates, protection in the upper respiratory tract appeared less robust than protection in the lower respiratory tract (Corbett et al., 2020; Mercado et al., 2020; van Doremalen et al., 2020; Yu et al., 2020). These data have raised the possibility that protection against asymptomatic infection may be more difficult to achieve than protection against severe pneumonia in humans. However, the role of vaccine dose in protection in the upper and lower respiratory tracts has not previously been defined. Moreover, suboptimal vaccine doses can be utilized to assess the theoretical concern of vaccine-associated enhanced respiratory disease (VAERD), although VAERD has not been reported to date in SARS-CoV-2 vaccine studies in animals or humans.

In this study, we assessed the immunogenicity and protective efficacy of a titration of Ad26.COV2.S dose levels to evaluate immune correlates of protection, define the role of reduced vaccine doses in protecting different anatomic respiratory compartments, and assess the possibility of VAERD.

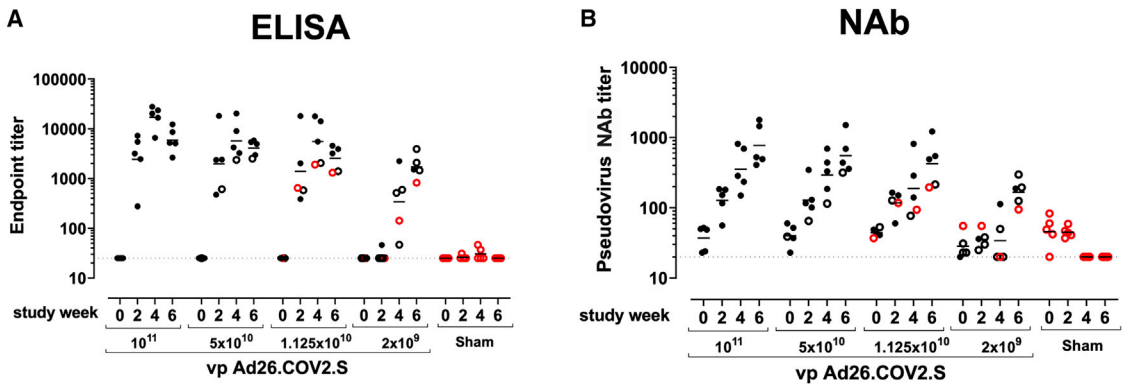

Figure 1. Humoral immune responses in vaccinated rhesus macaques

(A and B) Humoral immune responses were assessed at weeks 0, 2, 4, and 6 by (A) RBD-specific binding antibody ELISA and (B) pseudovirus neutralizing antibody (NAb) assays elicited by a single immunization of 1×10^{11}, 5×10^{10}, 1.125×10^{10}, or 2×10^{9} vp Ad26.COV2.S (n = 5/group) or sham negative controls (n = 10). Horizontal bars reflect geometric mean responses. Dotted lines reflect assay limit of quantitation. Solid black circles indicate animals that showed no virus in bronchoalveolar lavage (BAL) and nasal swabs (NSs) following challenge; open black circles indicate animals that showed virus in NSs, but not BAL, following challenge; and open red circles indicate animals that show virus in both BAL and NS following challenge.

See also Figures S1 and S2.

We observed that low doses of Ad26.COV2.S protected against Ad26.COV2.S challenge in the lower respiratory tract but that higher vaccine dose levels were required to protect in the upper respiratory tract. Suboptimal vaccine dose levels resulted in reduced protective efficacy, but no evidence of VAERD was observed.

RESULTS

Vaccine immunogenicity with reduced Ad26.COV2.S dose levels

We immunized 30 adult male and female rhesus macaques with a single dose of 1×10^{11}, 5×10^{10}, 1.125×10^{10}, or 2×10^{9} viral particles (vp) Ad26.COV2.S (n = 5/group) or sham (n = 10) at week 0 (Figure S1). We observed induction of receptor binding domain (RBD)-specific binding antibodies by ELISA in animals that received the 1×10^{11}, 5×10^{10}, and 1.125×10^{10} vp doses by week 2 and animals that received the 2×10^{9} vp dose by week 4 (Figure 1A). NAb responses were assessed using a pseudovirus neutralization assay (Chandrashekar et al., 2020; Yang et al., 2004; Yu et al., 2020) and were observed in the majority of animals in the three higher dose groups by week 2, with increasing titers through week 6 (Figure 1B). NAb titers remained low in the 2×10^{9} vp group at weeks 2 and 4 but became detectable in all animals by week 6, suggesting slower kinetics and lower magnitude NAb responses (Figure 1B). NAb responses at week 6 were 2.5-fold lower against the B.1.1.7 variant but were 3.4-fold lower against the B.1.351 variant (Figure S2).

Interferon-γ (IFN-γ) ELISpot assays using pooled S peptides demonstrated T cell responses in the majority of vaccinated animals that received the 1×10^{11}, 5×10^{10}, and 1.125×10^{10} vp doses at week 4, although there was a trend for lower responses with lower vaccine doses (Figure 2A). In animals that received the 2×10^{9} vp dose, only two out of five animals developed detectable ELISpot responses (Figure 2A). Interleukin-4 (IL-4) ELISpot responses were undetectable (Figure 2B), suggesting induction of T helper type 1 (Th1)-cell-biased responses and consistent with prior findings (Mercado et al., 2020).

We next monitored B cell responses following vaccination by multiparameter flow cytometry. SARS-CoV-2 RBD-specific IgG^{+} B cells were detected in peripheral blood by week 2 following vaccination and generally expressed the activation marker CD95 and the memory marker CD27 (Figure S3), suggesting activated memory B cells (Koutsakos et al., 2018; Neumann et al., 2015; Titanji et al., 2010). RBD-specific activated memory B cells expanded following vaccination in a dose-dependent fashion, with robust responses in animals that received 1×10^{11} vp but marginal responses in animals that received 2×10^{9} vp (Figure 3). The frequency of RBD-specific activated memory B cells strongly correlated with NAb and ELISA titers ($p < 0.0001$, $R = 0.7997$ and $p < 0.0001$, $R = 0.8851$, respectively, two-sided Spearman rank-correlation tests) and moderately correlated with IFN-γ ELISpot responses ($p = 0.0063$, $R = 0.5310$) (Figure S4).

Protective efficacy with reduced Ad26.COV2.S dose levels

We challenged all animals at week 6 with 1.0×10^{5} TCID50 SARS-CoV-2 by the intranasal (IN) and intratracheal (IT) routes (Chandrashekar et al., 2020; McMahan et al., 2021; Mercado et al., 2020; Yu et al., 2020). We assessed viral loads in bronchoalveolar lavage (BAL) and nasal swabs (NSs) by RT-PCR specific for subgenomic mRNA (sgRNA), which is believed to measure replicating virus (Chandrashekar et al., 2020; Wolfel et al., 2020). All 10 sham controls were infected and showed a mean peak of 4.45 (range, 3.2–6.5) $\log_{10}$ sgRNA copies/mL in BAL (Figure 4A). In contrast, vaccinated animals demonstrated no detectable virus in BAL (limit of quantitation, 1.69 $\log_{10}$ sgRNA copies/mL), with the exception of one animal in the 2×10^{9} vp group and one animal in the 1.125×10^{10} vp group (Figure 4A). Similarly, all sham controls showed a mean peak of 5.68 (range, 3.8–6.9) $\log_{10}$ sgRNA in NSs (Figure 4B). In contrast with limited

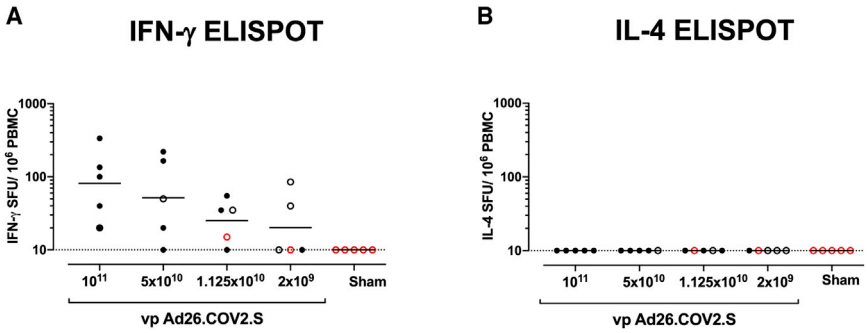

Figure 2. T cell responses in vaccinated rhesus macaques

(A and B) Cellular immune responses were assessed at week 4 following immunization by (A) IFN-γ and (B) IL-4 ELISpot assays in response to pooled S peptides. Horizontal bars reflect geometric mean responses. Dotted lines reflect assay limit of quantitation. Solid black circles indicate animals that showed no virus in BAL and NSs following challenge; open black circles indicate animals that showed virus in NSs, but not BAL, following challenge; and open red circles indicate animals that show virus in both BAL and NSs following challenge.

viral breakthroughs in the BAL, 80% (4 of 5) of animals in the 2 × 10^9 vp group, 40% (2 of 5) of animals in the 1.125 × 10^{10} vp group, and 20% (1 of 5) of animals in the 5 × 10^{10} vp group showed viral breakthroughs in NSs (Figure 4B). These data suggest that a higher vaccine dose may be required for protection in the upper respiratory tract compared with protection in the lower respiratory tract. Suboptimal vaccine dose levels led to loss of protection in NSs but did not result in enhanced virus replication compared with the sham controls.

The $\log_{10}$ ELISA and NAb titers at week 6 inversely correlated with peak $\log_{10}$ sgRNA in BAL ($p < 0.0001$, $R = -0.8489$ and $p < 0.0001$, $R = -0.8343$, respectively, two-sided Spearman rank-correlation tests; Figure 5) and NSs ($p < 0.0001$, $R = -0.7765$ and $p < 0.0001$, $R = -0.8436$, respectively, two-sided Spearman rank-correlation tests; Figure 5). Moreover, the frequency of RBD- and S-specific activated memory B cells inversely correlated with peak $\log_{10}$ sgRNA in NS ($p < 0.0001$, $R = -0.7196$ and $p = 0.0003$, $R = -0.6686$, respectively, for day 14 responses; $p = 0.0001$, $R = -0.6936$ and $p = 0.0014$, $R = -0.6039$, respectively, for day 28 responses; two-sided Spearman rank-correlation tests; Figure 6A). In addition, RBD- and S-specific activated memory B cells were higher in completely protected animals compared with partially protected or nonprotected animals ($p = 0.0006$ and $p = 0.0005$, two-sided Mann-Whitney tests; Figure 6B). Taken together, these data show that both memory B cell responses and binding or neutralizing antibody titers correlated with protection against SARS-CoV-2 in rhesus macaques.

Histopathology following SARS-CoV-2 challenge

On day 10 following challenge, animals were necropsied, and lung tissues were assessed by histopathology and immunohistochemistry. We observed focal to locally extensive SARS-CoV-2-associated pathological lesions in sham controls (Figure 7A; Table S1). We previously reported histopathologic evidence of

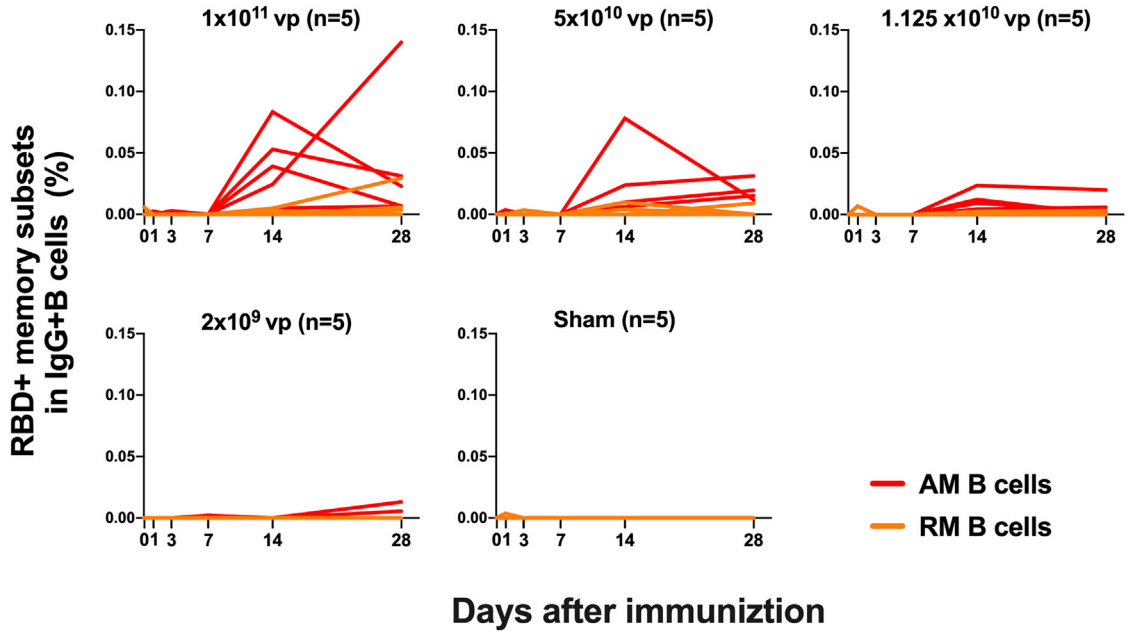

Figure 3. B cell responses in vaccinated rhesus macaques

Frequencies of RBD-specific $CD27^+CD95^+$ activated memory B cells (red) and resting memory B cells (orange) in total IgG^+ B cell populations on days 0, 1, 3, 7, 14, and 28 following Ad26.COV2.S or sham immunization. See also Figures S3 and S4.

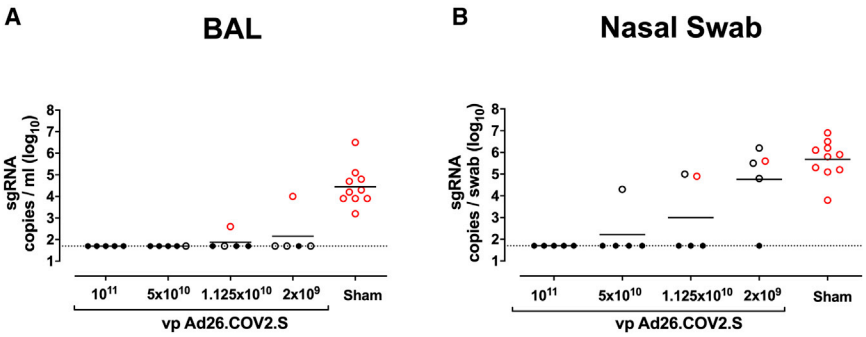

Figure 4. Protective efficacy following SARS-CoV-2 challenge

Rhesus macaques were challenged by the intranasal and intratracheal routes with 1.0 × 10^5 TCID50 SARS-CoV-2.

(A) Peak $\log_{10}$ sgRNA copies/mL (limit of quantification 50 copies/mL) were assessed in BAL following challenge.

(B) Peak $\log_{10}$ sgRNA copies/swab (limit of quantification 50 copies/swab) were assessed in NSs following challenge. Horizontal lines reflect geometric mean values. Solid black circles indicate animals that showed no virus in BAL and NS following challenge; open black circles indicate animals that showed virus in NSs, but not BAL, following challenge; and open red circles indicate animals that show virus in both BAL and NSs following challenge.

viral pneumonia in rhesus macaques on days 2 and 4 following SARS-CoV-2 infection (Chandrashekar et al., 2020). On day 10, lungs in sham controls still showed evidence of multifocal interstitial pneumonia with bronchoepithelial syncytia, perivascular mononuclear infiltrates, type II pneumocyte hyperplasia, rare thrombosis, and focal edema and consolidation (Figure S5; Table S1). RNAscope demonstrated *in situ* hybridization for viral RNA, immunohistochemistry showed staining for SARS nucleocapsid, and infiltrates included Iba-1$^+$ macrophages, CD3$^+$ T cells, and CD20$^+$ B cells (Figure S6). In contrast, vaccinated animals showed minimal histopathologic changes, consistent with background lung pathology, although several animals that received the 2 × 10^9 vp dose showed evidence of mild inflammation (Figure 7B; Table S1). No evidence of VAERD was observed in animals that received high or suboptimal doses of Ad26.COV2.S, including animals that showed breakthrough viral replication in BAL and/or NSs.

DISCUSSION

In this study, we demonstrate that low doses of the Ad26.COV2.S vaccine protected rhesus macaques against SARS-CoV-2 challenge, although higher vaccine doses were required to protect in the upper respiratory tract as compared with the lower respiratory tract. Both activated memory B cells and binding or neutralizing antibody titers correlated with protective efficacy. Suboptimal vaccine dose levels led to viral breakthroughs in the upper respiratory tract, but no virologic, immunologic, histopathologic, or clinical evidence of VAERD was observed.

These data confirm and extend prior studies in which we showed that single-shot immunization with Ad26.COV2.S effectively protected against SARS-CoV-2 infection in rhesus macaques and against severe clinical disease in hamsters (Mercado et al., 2020; Tostanoski et al., 2020). In the present study, we showed that Ad26.COV2.S doses as low as 2 × 10^9 vp

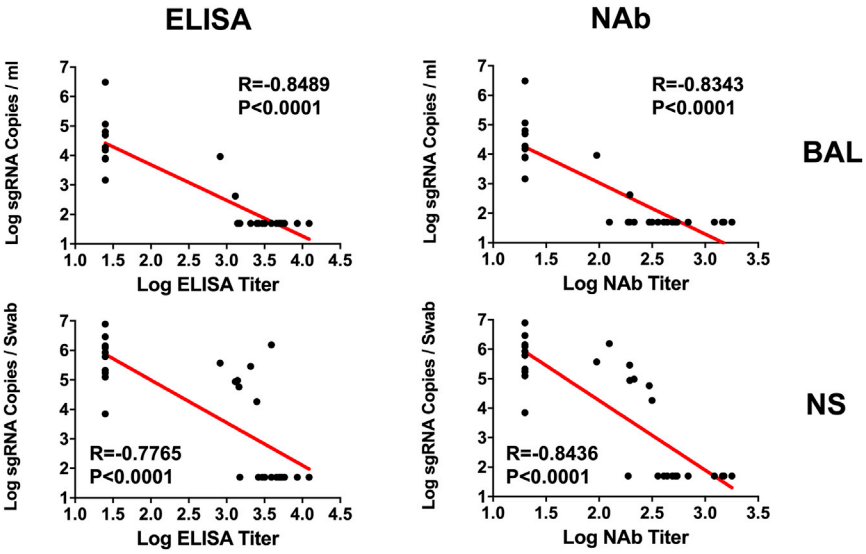

Figure 5. Antibody correlates of protection in BAL and NS

Correlations of log ELISA titers and log NAb titers at week 6 following vaccination with log peak sgRNA copies/mL in BAL and NSs following challenge. Red lines reflect the best linear fit relationship between these variables. p and R values reflect two-sided Spearman rank-correlation tests. n = 30 biologically independent animals.

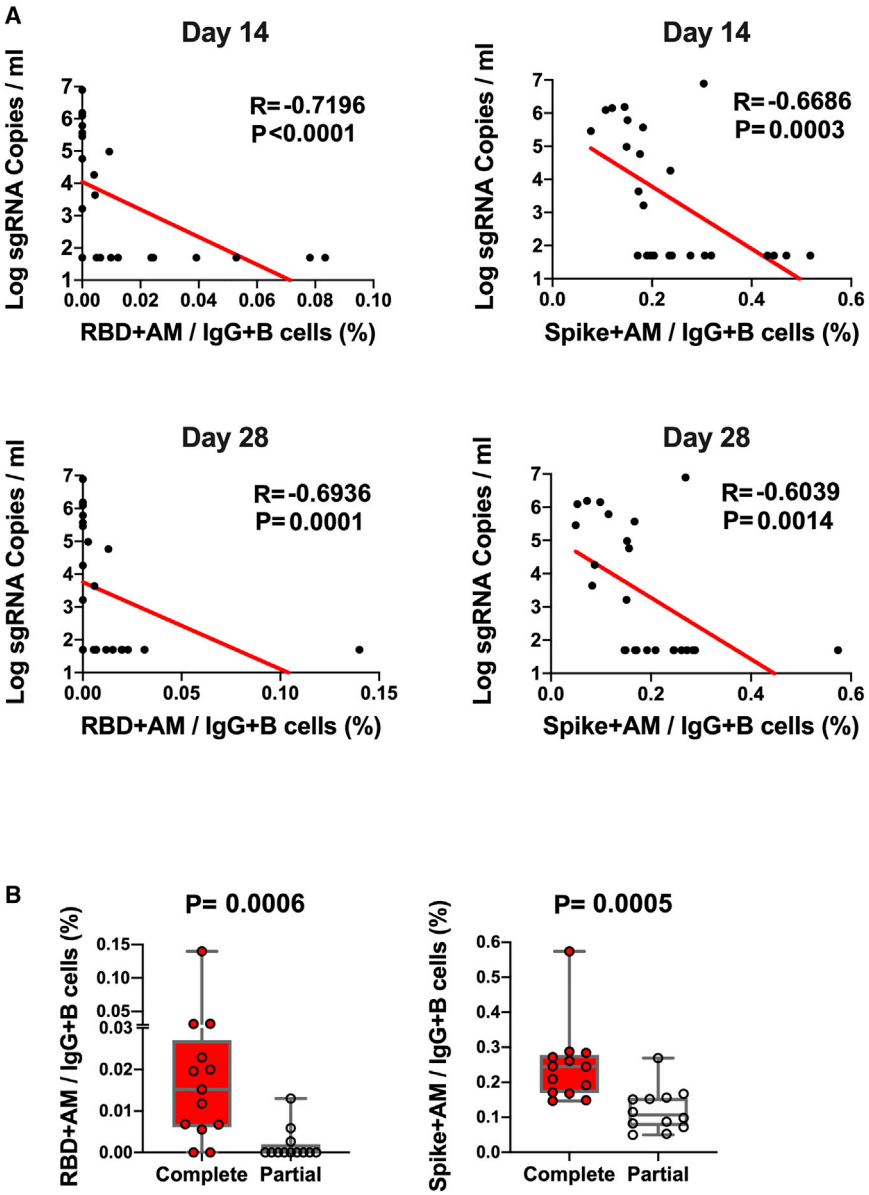

Figure 6. B cell correlates of protection in NSs

(A) Correlations of RBD- and S-specific activated memory B cell responses at days 14 and 28 following vaccination with log peak sgRNA copies/mL in NSs following challenge. Red lines reflect the best linear fit relationship between these variables. p and R values reflect two-sided Spearman rank-correlation tests. n = 25 biologically independent animals.

(B) Frequencies of RBD- and S-specific activated memory B cells in completely protected macaques (n = 13) and partially protected and non-protected macaques (n = 12). p values reflect two-sided Mann-Whitney tests.

protected the lower respiratory tract, whereas doses of 1.125×10^{10} vp were required to protect the upper respiratory tract. This anatomic-specific difference in protective efficacy is consistent with multiple SARS-CoV-2 vaccine studies in non-human primates using DNA, RNA, and Ad-vector-based vaccines, which have consistently shown superior protection in the lungs compared with the nasal cavity (Corbett et al., 2020; Mercado et al., 2020; van Doremalen et al., 2020; Yu et al., 2020). These findings suggest that future work evaluating mucosal immune responses in these anatomic compartments is warranted. Future work also will need to evaluate receptor density in the upper and lower respiratory tract.

Previous studies have suggested that vaccine-elicited binding and neutralizing antibodies correlated with protection against SARS-CoV-2 in rhesus macaques (Mercado et al., 2020; Yu et al., 2020) and that adoptive transfer of purified IgG from convalescent macaques protected against SARS-CoV-2 in this model (McMahan et al., 2021). The present data are consistent with these prior observations, and both RBD-specific activated memory B cells and binding or neutralizing antibody responses correlated with protective efficacy. Moreover, lower vaccine doses led to diminished antibody responses and reduced protective efficacy, further suggesting the importance of humoral immunity in protection against SARS-CoV-2. Suboptimal vaccine dose levels led to viral breakthroughs but did not result in enhanced viral replication or increased pathology in the lungs of vaccinated animals compared with sham controls, although other mechanisms may also contribute to enhanced disease.

In summary, our data demonstrate that a single immunization of low-dose Ad26.COV2.S protects against SARS-CoV-2 challenge in rhesus macaques. Low-dose vaccination led to viral breakthrough in the upper respiratory tract prior to the lower respiratory tract, raising the possibility that SARS-CoV-2 vaccines may protect against severe pneumonia more effectively than against mild disease or asymptomatic infection in humans. However, these findings in macaques will need to be evaluated in humans. To this end, two phase 3 trials are currently in progress to determine the safety and efficacy of Ad26.COV2.S in humans, including against variants of concern. Ad26.COV.2 has recently received US Food and Drug Administration (FDA) emergency use authorization for prevention of coronavirus disease 2019 (COVID-19) disease in humans.

Limitations of study

A key limitation of our study is that experiments in macaques may not fully model human vaccine immunogenicity and

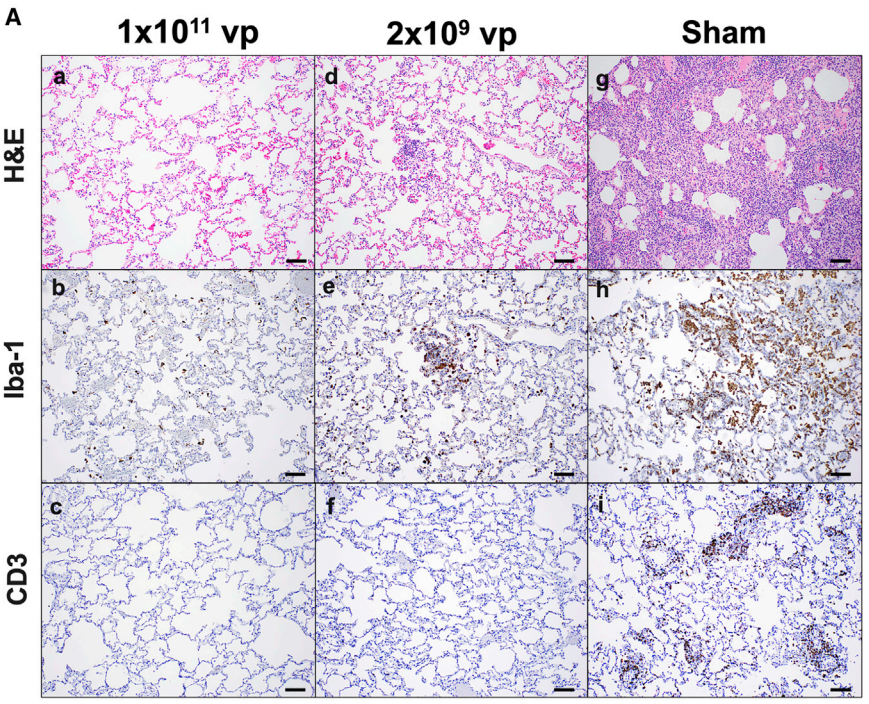

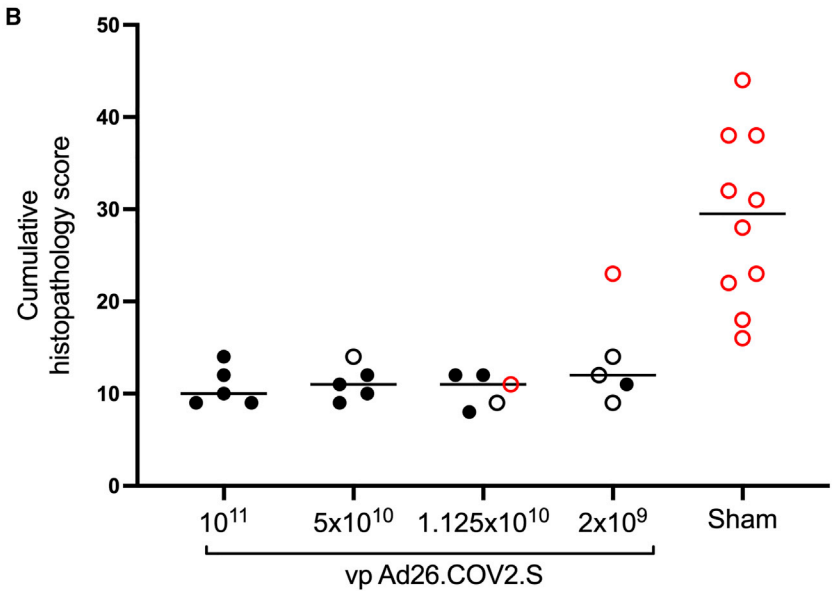

Figure 7. Comparative pathology in vaccinated and unvaccinated animals following SARS-CoV-2 challenge

(A) Representative pathology from animals vaccinated with (a–c) 1 × 10^{11} vp Ad26.COV2.S, (d–f) 2x10^{9} vp Ad26.COV2.S, or (g–i) sham negative controls on day 10 following SARS-CoV-2 challenge. (a, d, and g) representative H&E histopathology. (b, e, and h) immunohistochemistry for Iba-1 (macrophages). (c, f, and i) Immunohistochemistry for CD3 (T lymphocytes). Animals that received a high vaccine dose had minimal evidence of SARS-CoV-2 pathology (a–c). Animals that received the lowest vaccine dose showed focal pathology (d–f) characterized by increased alveolar macrophages, focal interstitial septal thickening, and aggregates of macrophages. Sham-vaccinated animals had locally extensive moderate interstitial pneumonia (g) characterized by extensive macrophage infiltrates (h) and expansion of perivascular and interstitial CD3 T lymphocytes (i).

(B) Histopathologic scoring of lung lesions in all lobes in vaccinated and sham animals following SARS-CoV-2 challenge. Scoring was performed independently by two blinded veterinary pathologists. Lesions reported included (1) inflammation interstitial/septal thickening; (2) infiltrate, macrophage; (3) alveolar infiltrate, mononuclear; (4) perivascular infiltrate, macrophage; (5) bronchiolar type II pneumocyte hyperplasia; (6) bronchus-associated lymphoid tissue (BALT) hyperplasia; (7) inflammation, bronchiolar/peribronchiolar infiltrate; (8) neutrophils, bronchiolar/alveolar; and (9) infiltrate, eosinophils. Lesions such as focal fibrosis and syncytia were reported, but not included in scoring. Edema, alveolar flooding was excluded from scoring since animals received terminal BALs. Each feature assessed was assigned a score (0 = no significant findings; 1 = minimal; 2 = mild; 3 = moderate; 4 = marked/severe). Eight representative samples from cranial, middle, and caudal lung lobes from the left and right lungs were evaluated from each animal and were scored independently. Scores were added for all lesions across all lung lobes for each animal for a maximum possible score of 288 for each monkey. Lungs evaluated were inflated/suffused with 10% formalin. Horizontal lines reflect median values. Solid black circles indicate animals that showed no virus in BAL and NS following challenge, open black circles indicate animals that showed virus in NS but not BAL following challenge, and open red circles indicate animals that show virus in both BAL and NS following challenge. Scale bars, 100 μm.

See also Figures S5 and S6 and Table S1.

efficacy. Our study is also limited by the small number of animals per group and the lack of correlations between mucosal immune responses and protective efficacy.

STAR★METHODS

Detailed methods are provided in the online version of this paper and include the following:

- KEY RESOURCES TABLE
- RESOURCE AVAILABILITY
  - Lead contact
  - Materials availability
  - Data and code availability
- EXPERIMENTAL MODEL AND SUBJECT DETAILS
  - Animals and study design
- METHOD DETAILS

- Subgenomic mRNA assay
- Enzyme-linked immunosorbent assay (ELISA)
- Pseudovirus neutralization assay
- IFN-γ enzyme-linked immunospot (ELISpot) assay
- IL-4 ELISpot assay
- B cell immunophenotyping
- Histopathology and immunohistochemistry
- RNAscope

● QUANTIFICATION AND STATISTICAL ANALYSIS

SUPPLEMENTAL INFORMATION

Supplemental information can be found online at https://doi.org/10.1016/j.cell.2021.05.040.

ACKNOWLEDGMENTS

We thank M. Gebre, K. Verrington, E. Hoffman, L. Wrijil, T. Hayes, and K. Bauer for generous advice, assistance, and reagents. This project was funded in part by the Department of Health and Human Services Biomedical Advanced Research and Development Authority (BARDA) under contract HHS0100201700018C. We also acknowledge support from Janssen Vaccines & Prevention BV; the Ragon Institute of MGH, MIT, and Harvard; the Mark and Lisa Schwartz Foundation; the Massachusetts Consortium on Pathogen Readiness (MassCPR); the National Institutes of Health (CA260476, OD024917, AI135098, AI129797, AI128751, AI126603, and AI124377); and Fast Grants, Emergent Ventures, Mercatus Center at George Mason University.

AUTHOR CONTRIBUTIONS

D.H.B., R.Z., F.W., S.R.H., M.v.H., L.v.d.F., and H.S. designed the study and reviewed all data. X.H., A. Chandrashekar, J.Y., N.B.M., K.M., E.N.B., M.L., J.L., F.N., S.P., L. Peter, and L.H.T. performed the immunologic and virologic assays. A.J.M., C.P.-M., S.B., S.D., and R.C. performed the pathologic analyses. L. Pessaint, A.V.R., B.F., J.V., E.T., R.B., A. Cook, H.A., and M.G.L. led the clinical care of the animals. D.H.B. wrote the paper with all co-authors.

DECLARATION OF INTERESTS

D.H.B., R.Z., F.W., and H.S are co-inventors on provisional vaccine patents (63/121,482; 63/133,969; 63/135,182). R.Z., F.W., S.R.H., M.v.H., L.v.d.F., and H.S. are employees of Janssen Vaccines & Prevention BV and may hold stock in Johnson & Johnson.

Received: February 2, 2021
Revised: March 18, 2021
Accepted: May 25, 2021
Published: June 1, 2021

REFERENCES

Abbink, P., Lemckert, A.A., Ewald, B.A., Lynch, D.M., Denholtz, M., Smits, S., Holterman, L., Damen, I., Vogels, R., Thorner, A.R., et al. (2007). Comparative seroprevalence and immunogenicity of six rare serotype recombinant adenovirus vaccine vectors from subgroups B and D. J. Virol. *81*, 4654–4663.

Bos, R., Rutten, L., van der Lubbe, J.E.M., Bakkers, M.J.G., Hardenberg, G., Wegmann, F., Zuijdgeest, D., de Wilde, A.H., Koornneef, A., Verwilligen, A., et al. (2020). Ad26 vector-based COVID-19 vaccine encoding a prefusion-stabilized SARS-CoV-2 Spike immunogen induces potent humoral and cellular immune responses. NPJ Vaccines *5*, 91.

Chandrashekar, A., Liu, J., Martinot, A.J., McMahan, K., Mercado, N.B., Peter, L., Tostanoski, L.H., Yu, J., Maliga, Z., Nekorchuk, M., et al. (2020). SARS-CoV-2 infection protects against rechallenge in rhesus macaques. Science *369*, 812–817.

Corbett, K.S., Flynn, B., Foulds, K.E., Francica, J.R., Boyoglu-Barnum, S., Werner, A.P., Flach, B., O'Connell, S., Bock, K.W., Minai, M., et al. (2020). Evaluation of the mRNA-1273 Vaccine against SARS-CoV-2 in Nonhuman Primates. N. Engl. J. Med. *383*, 1544–1555.

Gao, Q., Bao, L., Mao, H., Wang, L., Xu, K., Yang, M., Li, Y., Zhu, L., Wang, N., Lv, Z., et al. (2020). Development of an inactivated vaccine candidate for SARS-CoV-2. Science *369*, 77–81.

Koutsakos, M., Wheatley, A.K., Loh, L., Clemens, E.B., Sant, S., Nüssing, S., Fox, A., Chung, A.W., Laurie, K.L., Hurt, A.C., et al. (2018). Circulating T_{FH} cells, serological memory, and tissue compartmentalization shape human influenza-specific B cell immunity. Sci. Transl. Med. *10*, eaan8405.

McMahan, K., Yu, J., Mercado, N.B., Loos, C., Tostanoski, L.H., Chandrashekar, A., Liu, J., Peter, L., Atyeo, C., Zhu, A., et al. (2021). Correlates of protection against SARS-CoV-2 in rhesus macaques. Nature *590*, 630–634.

Mercado, N.B., Zahn, R., Wegmann, F., Loos, C., Chandrashekar, A., Yu, J., Liu, J., Peter, L., McMahan, K., Tostanoski, L.H., et al. (2020). Single-shot Ad26 vaccine protects against SARS-CoV-2 in rhesus macaques. Nature *586*, 583–588.

Neumann, B., Klippert, A., Raue, K., Sopper, S., and Stahl-Hennig, C. (2015). Characterization of B and plasma cells in blood, bone marrow, and secondary lymphoid organs of rhesus macaques by multicolor flow cytometry. J. Leukoc. Biol. *97*, 19–30.

Titanji, K., Velu, V., Chennareddi, L., Vijay-Kumar, M., Gewirtz, A.T., Freeman, G.J., and Amara, R.R. (2010). Acute depletion of activated memory B cells involves the PD-1 pathway in rapidly progressing SIV-infected macaques. J. Clin. Invest. *120*, 3878–3890.

Tostanoski, L.H., Wegmann, F., Martinot, A.J., Loos, C., McMahan, K., Mercado, N.B., Yu, J., Chan, C.N., Bondoc, S., Starke, C.E., et al. (2020). Ad26 vaccine protects against SARS-CoV-2 severe clinical disease in hamsters. Nat. Med. *26*, 1694–1700.

van Doremalen, N., Lambe, T., Spencer, A., Belij-Rammerstorfer, S., Purushotham, J.N., Port, J.R., Avanzato, V.A., Bushmaker, T., Flaxman, A., Ulaszewska, M., et al. (2020). ChAdOx1 nCoV-19 vaccine prevents SARS-CoV-2 pneumonia in rhesus macaques. Nature *586*, 578–582.

Wang, H., Zhang, Y., Huang, B., Deng, W., Quan, Y., Wang, W., Xu, W., Zhao, Y., Li, N., Zhang, J., et al. (2020). Development of an Inactivated Vaccine Candidate, BBIBP-CorV, with Potent Protection against SARS-CoV-2. Cell *182*, 713–721.e9.

Wolfel, R., Corman, V.M., Guggemos, W., Seilmaier, M., Zange, S., Muller, M.A., Niemeyer, D., Jones, T.C., Vollmar, P., Rothe, C., et al. (2020). Virological assessment of hospitalized patients with COVID-2019. Nature *581*, 465–469.

Wrapp, D., Wang, N., Corbett, K.S., Goldsmith, J.A., Hsieh, C.L., Abiona, O., Graham, B.S., and McLellan, J.S. (2020). Cryo-EM structure of the 2019-nCoV spike in the prefusion conformation. Science *367*, 1260–1263.

Yang, Z.Y., Kong, W.P., Huang, Y., Roberts, A., Murphy, B.R., Subbarao, K., and Nabel, G.J. (2004). A DNA vaccine induces SARS coronavirus neutralization and protective immunity in mice. Nature *428*, 561–564.

Yu, J., Tostanoski, L.H., Peter, L., Mercado, N.B., McMahan, K., Mahrokhian, S.H., Nkolola, J.P., Liu, J., Li, Z., Chandrashekar, A., et al. (2020). DNA vaccine protection against SARS-CoV-2 in rhesus macaques. Science *369*, 806–811.

Yu, J., Li, Z., He, X., Gebre, M.S., Bondzie, E.A., Wan, H., Jacob-Dolan, C., Martinez, D.R., Nkolola, J.P., Baric, R.S., et al. (2021). Deletion of the SARS-CoV-2 Spike Cytoplasmic Tail Increases Infectivity in Pseudovirus Neutralization Assays. J. Virol. Published online March 16, 2021. https://doi.org/10.1128/JVI.00044-21.

STAR★METHODS

KEY RESOURCES TABLE

REAGENT or RESOURCE	SOURCE	IDENTIFIER
Antibodies		
Mouse anti-human IFN-γ monoclonal antibody	BD PharMingen	Cat # 554699; RRID:AB_398579
Rabbit polyclonal anti-human IFN-γ Biotin	U-Cytech	Cat # CT243
Streptavidin-alkaline phosphatase antibody	Southern Biotech	Cat # 7100-04
Mouse anti-human Ki-67 PerCP-cy5.5	BD PharMingen	Cat # 561284; RRID:AB_10611574
Goat anti-human IgD PE	Southern Biotec	Cat # 2030-09; RRID:AB_2795630
Mouse anti-human CD138 PE-CF594	BIOLEGEND	Cat # 352320 RRID:AB_2687342
Mouse anti-human CD20 PE-Cy5	BD PharMingen	Cat # 555624; RRID:AB_395990
Rat anti-human IRF4 PE Cy7	Affymetrix	Cat # 25-9858-82; RRID:AB_2573558
Mouse anti-human CD14 BV570	BIOLEGEND	Cat # 301832; RRID:AB_2563629
Mouse anti-human CD21 BV605	BD PharMingen	Cat # 740395; RRID:AB_2740125
Mouse anti-human CD95 BV711	BIOLEGEND	Cat # 305644; RRID:AB_2632623
Mouse anti-human CD80 BV786	BD PharMingen	Cat # 564159; RRID:AB_2738631
Mouse anti-human IgM BUV395	BD PharMingen	Cat # 563903; RRID:AB_2721269
Mouse anti-human CD27 BUV563	BD PharMingen	Cat # 741366; RRID:AB_2870866
Mouse anti-human IgG BUV737	BD PharMingen	Cat # 612819; RRID:AB_2870143
Mouse anti-human CD45 BUV805	BD PharMingen	Cat # 742055; RRID:AB_2871344
Goat anti-human IgA APC	FISHER/JACKSON	Cat # 109-135-011; RRID:AB_2337689
Mouse anti-human CD11c Alexa700	Affymetrix	Cat # 56-0116-42; RRID:AB_10547281
Mouse anti-human CD123 Alexa700	FISHER/NOVUS	Cat # NB6001185AF700
Mouse anti-human CD7 Alexa700	BD PharMingen	Cat # 561603; RRID:AB_10898348
Mouse anti-human CD3 APC-Cy7	BD PharMingen	Cat # 557757; RRID:AB_396863
Anti-macaque IgG HRP	Nonhuman Primate Reagent Resource	Cat# 1b3-HRP; 0320K235 / 070920SC
Rabbit polyclonal anti-SARS-NN	Novus	Cat# NB100-56576; RRID:AB_838838:
Rabbit anti-CD3 antibody	Sigma	Cat# SAB5500057
Rabbit polyclonal anti-Iba-1	Wako	Cat# 019-19741; RRID:AB_839504
Rabbit anti-CD20 antibody	Invitrogen	Cat# PA5-16701; RRID:AB_10980806
Bacterial and virus strains		
SARS-CoV-2	BEI Repository	Isolate: USA-WA1/2020
Biological samples		
Non-human primate SARS-CoV2 infected lung tissue, fixed, embedded	Bioqual	N/A
Bronchoalveolar lavage from Non-Human Primates	Bioqual	N/A
Nasal swabs from Non-Human Primates	Bioqual	N/A
EDTA, SST, Paxgene collection tubes with whole blood, from Non-Human Primates	Bioqual	N/A
Chemicals, peptides, and recombinant proteins		
nCOV Spike Pool 1	JPT	Custom
nCOV Spike Pool 2	JPT	Custom
Nitorblue Tetrazolium Chloride/5-bromo-4-chloro 3 'indolyl phosphate p-toludine salt	Thermo Scientific	Cat #34042

(*Continued on next page*)

Continued

REAGENT or RESOURCE	SOURCE	IDENTIFIER
Biotinylated SARS-CoV-2 RBD proteins	Sino Biological	Cat # 40592-V08B-B
Full-length SARS-CoV-2 spike proteins	Sino Biological	Cat # 40589-V08B1
BV650 streptavidin	BD PharMingen	Cat # 563855; RRID:AB_2869528
Fixation Medium (Medium A)	ThermoFisher Scientific	Cat # GAS001S100
Permeabilization Medium (Medium B)	ThermoFisher Scientific	Cat # GAS002S100
SARS-CoV-2 Receptor Binding Domain protein	Aaron Schmidt Laboratory; Harvard Medical School	https://doi.org/10.1126/sciimmunol.abe0367
Full-length SARS-CoV-2 Spike protein	Bing Chen Laboratory; Harvard Medical Schol	https://doi.org/10.1126/science.abd4251
Critical commercial assays		
Human IL-4 ELISpot^{PRO} Kit	MABTECH	3410-2APW-2
Rabbit Mach-2 HRP-Polymer	Biocare	RHRP520L
SARS-CoV2 anti-sense specific probe v-nCoV2019-S	ACD	Cat# 848561
RNAscope 2.5 HD Detection Reagents-RED	ACD	Cat# 322360
Experimental models: cell lines		
HEK293T-hACE2	This paper	N/A
Experimental models: organisms/strains		
Macaca mulatta	https://www.unmc.edu/rhesusgenechip/index.htm	https://www.unmc.edu/rhesusgenechip/index.htm
Oligonucleotides		
Primer:sgLeadSARSCoV2-F Forward: CGATCTCTTGTAGATCTGTTCTC	Wolfel et al., 2020	ThermoFisher Scientific:4448510
Primer: E_Sarbeco_R Reverse: ATATTGCAGCAGTACGCACACA	Wolfel et al., 2020	ThermoFisher Scientific:4448510
Probe:E_Sarbeco_P1: VIC-ACACTAG CCATCCTTACTGCGCTTCG-MGBNFQ	Wolfel et al., 2020	ThermoFisher Scientific:4448510
Primer:pcDNA.T7.NdeI.Fwd Forward: TG ATCTCATATGGAACCCACTGCTTACTG	This paper	Integrated DNA Technologies
Primer: pcDNA.T7.Rev Reverse: CACTGTGCTGGATATCTGC	This paper	Integrated DNA Technologies
Recombinant DNA		
psPAX2	AIDS Resource and Reagent Program	Cat# 11348
pLenti-CMV Puro-Luc	Addgene	Cat# 17477
pcDNA3.1-SARS CoV-2 SΔCT	This paper	N/A
Plasmid: pcDNA3.1+. SARS-CoV-2 E gene subgenomic RNA (sgRNA)	This paper	N/A
Software and algorithms		
GraphPad Prism 8.4.2	GraphPad Software	https://www.graphpad.com/scientific-software/prism/
FlowJo software 9.9.6	BD Bioscience	https://www.flowjo.com/
QuantStudio Real-Time PCR Software v1.7.1	Life Technologies	https://www.thermofisher.com/us/en/home/global/forms/life-science/quantstudio-6-7-flex-software.html
SoftMax Pro 6.5.1	SoftMax Pro Software	https://www.moleculardevices.com/products/microplate-readers/acquisition-and-analysis-software/softmax-pro-software
BioRender	BioRender	https://biorender.com/

(*Continued on next page*)

Continued

REAGENT or RESOURCE	SOURCE	IDENTIFIER
Other		
Ad26.COV2.S	Janssen	JNJ-78436735
RNA Standard: SARS-CoV-2 E gene subgenomic RNA (sgRNA)	This paper	N/A

RESOURCE AVAILABILITY

Lead contact

Further information and requests for resources and reagents should be directed to and will be fulfilled by the Lead Contact, Dr. Dan Barouch (dbarouch@bidmc.harvard.edu).

Materials availability

This study did not generate new unique reagents.

Data and code availability

There is no dataset/code associated with the paper.

EXPERIMENTAL MODEL AND SUBJECT DETAILS

Animals and study design

30 outbred Indian-origin adult male (10) and female (20) rhesus macaques (*Macaca mulatta*) were randomly allocated to groups. Animals were 5-8 kg. All animals were housed at Bioqual, Inc. (Rockville, MD). Animals received a single immunization of $1x10^{11}$, $5x10^{10}$, $1.125x10^{10}$, or $2x10^{9}$ viral particles (vp) Ad26.COV2.S (Janssen; n = 5/group) or sham (n = 10) by the intramuscular route without adjuvant at week 0. At week 6, all animals were challenged with $1.0x10^{5}$ TCID50 ($1.2x10^{8}$ RNA copies, $1.1x10^{4}$ PFU) SARS-CoV-2, which was derived from USA-WA1/2020 (NR-52281; BEI Resources) and deep sequenced (Chandrashekar et al., 2020). Virus was administered as 1 mL by the intranasal (IN) route (0.5 mL in each nare) and 1 mL by the intratracheal (IT) route. All immunologic, virologic, and histopathologic studies were performed as blinded studies. Animal studies were conducted in compliance with all relevant local, state, and federal regulations and were approved by the Bioqual Institutional Animal Care and Use Committee (IACUC).

METHOD DETAILS

Subgenomic mRNA assay

In order to quantify viral load levels from macaque bronchoalveolar lavage (BAL) fluid and nasal swabs (NS), RNA was first isolated from 200ul of sample. The samples were heat inactivated for 30 minutes at 56°C then 100ul of lysis buffer/carrier RNA provided by the IndiSpin QIAcube HT Pathogen Kit (Indical Bioscience) was added to each sample. RNA extraction was performed on a QIAcube HT using the IndiSpin QIAcube HT Pathogen Kit according to manufacturer's specifications. Post extraction, 25ul of RNA was reverse transcribed to cDNA using Superscript VILO (Invitrogen). The master mix for reverse transcription was as follows, 10ul of UltraPure DNase/RNase-Free Distilled Water, 10ul of SuperScript VILO Master Mix, and 25ul of RNA template. The cycling conditions for reverse transcription were, 25°C for 10 minutes, 42°C for 1 hour then 85°C for 5 minutes. cDNA was stored at 4°C until RT-PCR assays were performed. A Taqman custom gene expression assay (ThermoFisher Scientific) was designed using the sequences targeting the E gene sgRNA (Wolfel et al., 2020). The sequences for the custom assay were as follows, forward primer:sgLeadCoV2.Fwd: CGATCTCTTGTAGATCTGTTCTC, E_Sarbeco_R: ATATTGCAGCAGTACGCACACA, E_Sarbeco_P1 (probe): VIC-ACACTAGCCATCCTTACTGCGCTTCG-MGB. Reactions were carried out in duplicate for samples and standards on the QuantStudio 6 and 7 Flex Real-Time PCR Systems (Applied Biosystems) with the thermal cycling conditions, initial denaturation at 95°C for 20 s, then 45 cycles of 95°C for 1 s and 60°C for 20 s. For all RT-PCR runs the following quality control (QC) acceptance range for standard curves must be met: $R2 > 0.98$, efficiency 90 to 110%, and slope $-3.1 < x > -3.6$. Analysis was performed on the QuantStudio Real-Time PCR Software (Life Technologies). Standard curves were used to calculate subgenomic RNA copies per ml or per swab; the quantitative assay sensitivity was 50 copies per ml or per swab.

Enzyme-linked immunosorbent assay (ELISA)

Binding antibodies were assessed by ELISA essentially as described (Chandrashekar et al., 2020; Yu et al., 2020). Briefly, 96-well plates were coated with 1 μg/ml SARS-CoV-2 spike (S) or receptor binding domain (RBD) protein in 1X DPBS and incubated at 4°C overnight. After incubation, plates were washed once with wash buffer (0.05% Tween 20 in 1 X DPBS) and blocked with

350 μL Casein block/well for 2-3 h at room temperature. After incubation, block solution was discarded and plates were blotted dry. Serial dilutions of heat-inactivated serum diluted in casein block were added to wells and plates were incubated for 1 h at room temperature, prior to three further washes and a 1 h incubation with a 1:1000 dilution of anti-macaque IgG HRP (NIH NHP Reagent Program) at room temperature in the dark. Plates were then washed three times, and 100 μL of SeraCare KPL TMB SureBlue Start solution was added to each well; plate development was halted by the addition of 100 μL SeraCare KPL TMB Stop solution per well. The absorbance at 450nm was recorded using a VersaMax or Omega microplate reader. ELISA endpoint titers were defined as the highest reciprocal serum dilution that yielded an absorbance > 0.2. Log10 endpoint titers are reported.

Pseudovirus neutralization assay

The SARS-CoV-2 pseudoviruses expressing a luciferase reporter gene were generated in an approach similar to as described previously (Chandrashekar et al., 2020; Yang et al., 2004; Yu et al., 2020, 2021). Briefly, the packaging plasmid psPAX2 (AIDS Resource and Reagent Program), luciferase reporter plasmid pLenti-CMV Puro-Luc (Addgene), and spike protein expressing pcDNA3.1-SARS CoV-2 SΔCT of variants were co-transfected into HEK293T cells by lipofectamine 2000 (ThermoFisher). Pseudoviruses of SARS-CoV-2 variants were generated by using Wuhan prototype strain (Wuhan/WIV04/2019, GISAID accession ID: EPI_ISL_402124), D614G mutation, B.1.1.7 variant (GISAID accession ID: EPI_ISL_601443), or B.1.351 variant (GISAID accession ID: EPI_ISL_712096). The supernatants containing the pseudotype viruses were collected 48 h post-transfection, which were purified by centrifugation and filtration with 0.45 μm filter. To determine the neutralization activity of the plasma or serum samples from participants, HEK293T-hACE2 cells were seeded in 96-well tissue culture plates at a density of 1.75×10^4 cells/well overnight. Three-fold serial dilutions of heat inactivated serum or plasma samples were prepared and mixed with 50 μL of pseudovirus. The mixture was incubated at 37°C for 1 h before adding to HEK293T-hACE2 cells. 48 h after infection, cells were lysed in Steady-Glo Luciferase Assay (Promega) according to the manufacturer's instructions. SARS-CoV-2 neutralization titers were defined as the sample dilution at which a 50% reduction in relative light unit (RLU) was observed relative to the average of the virus control wells.

IFN-γ enzyme-linked immunospot (ELISpot) assay

ELISpot plates were coated with mouse anti-human IFN-γ monoclonal antibody from BD PharMingen at a concentration of 5 μg/well overnight at 4°C, and assays were performed as described (Chandrashekar et al., 2020; Yu et al., 2020). Plates were washed with DPBS containing 0.25% Tween 20, and blocked with R10 media (RPMI with 11% FBS and 1.1% penicillin-streptomycin) for 1 h at 37°C. The Spike 1 and Spike 2 peptide pools contain 15 amino acid peptides overlapping by 11 amino acids that span the protein sequence and reflect the N- and C-terminal halves of the protein, respectively. Spike 1 and Spike 2 peptide pools were prepared at a concentration of 2 μg/well, and 200,000 cells/well were added. The peptides and cells were incubated for 18-24 h at 37°C. All steps following this incubation were performed at room temperature. The plates were washed with coulter buffer and incubated for 2 h with Rabbit polyclonal anti-human IFN-γ Biotin from U-Cytech (1 μg/mL). The plates are washed a second time and incubated for 2 h with Streptavidin-alkaline phosphatase antibody from Southern Biotechnology (1 μg/mL). The final wash was followed by the addition of Nitor-blue Tetrazolium Chloride/5-bromo-4-chloro 3 'indolyl phosphate p-toludine salt (NBT/BCIP chromagen) substrate solution for 7 min. The chromagen was discarded and the plates were washed with water and dried in a dim place for 24 h. Plates were scanned and counted on a Cellular Technologies Limited Immunospot Analyzer.

IL-4 ELISpot assay

Precoated monoclonal antibody IL-4 ELISpot plates (Mabtech) were washed and blocked. The assay was then performed as described above except the development time with NBT/BCIP chromagen substrate solution was 12 min.

B cell immunophenotyping

Fresh PBMCs were stained with Aqua live/dead dye for 20 min, washed with 2% FBS/DPBS buffer, and cells were suspended in 2% FBS/DPBS buffer with Fc Block (BD) for 10 min, followed by staining with monoclonal antibodies against CD45 (clone D058-1283, BUV805), CD3 (clone SP34.2, APC-Cy7), CD7 (clone M-T701, Alexa700), CD123 (clone 6H6, Alexa700), CD11c (clone 3.9, Alexa700), CD20 (clone 2H7, PE-Cy5), IgA (goat polyclonal antibodies, APC), IgG (clone G18-145, BUV737), IgM (clone G20-127, BUV395), IgD (goat polyclonal antibodies, PE), CD80 (clone L307.4, BV786), CD95 (clone DX2, BV711), CD27 (clone M-T271, BUV563), CD21 (clone B-ly4, BV605), CD14 (clone M5E2, BV570), CD138 (clone DL-101, PE-CF594), and staining with SARS-CoV-2 antigens including biotinylated SARS-CoV-2 RBD proteins (Sino Biological) and full-length SARS-CoV-2 spike proteins (Sino Biological) labeled with FITC and DyLight 405, at 4°C for 30 min. After staining, cells were washed twice with 2% FBS/DPBS buffer, followed by incubation with BV650 streptavidin (BD PharMingen) for 10min, then washed twice with 2% FBS/DPBS buffer. For intracellular staining, cells were permeabilized using Caltag Fix & Perm (ThermoFisher Scientific), then stained with monoclonal antibodies against Ki67 (clone B56, PerCP-cy5.5) and IRF4 (clone 3E4, PE-Cy7). After staining, cells were washed and fixed by 2% paraformaldehyde. All data were acquired on a BD FACSymphony flow cytometer. Subsequent analyses were performed using FlowJo software (BD Bioscience, v.9.9.6). For analyses, in singlet gate, dead cells were excluded by Aqua dye and CD45 was used as a positive inclusion gate for all leukocytes. Within class-switched B cell population gated as CD20+IgG+IgM-IgD-CD3-CD14-CD11c-CD123-CD7-, SARS-CoV-2 RBD-specific B cells were identified as double positive for SARS-CoV-2 RBD and spike proteins, and SARS-CoV-2 spike-specific B cells were identified as double positive for SARS-CoV-2 spike proteins labeled with different

fluorescent probes. The SARS-CoV-2-specific B cells were further distinguished according to CD21/CD27 phenotype distribution: activated memory B cells (CD21-CD27+) and resting memory B cells (CD21+CD27+).

Histopathology and immunohistochemistry

At time of fixation, lungs were suffused with 10% formalin to expand the alveoli. All tissues were fixed in 10% formalin and blocks sectioned at 5 μm. Slides were baked for 30-60 min at 65 degrees then deparaffinized in xylene and rehydrated through a series of graded ethanol to distilled water. Heat induced epitope retrieval (HIER) was performed using a pressure cooker on steam setting for 25 minutes in citrate buffer (Thermo; AP-9003-500) followed by treatment with 3% hydrogen peroxide. Slides were then rinsed in distilled water and protein blocked (BioCare, BE965H) for 15 min followed by rinses in 1x phosphate buffered saline. Primary rabbit anti-SARS-nucleoprotein antibody (Novus; NB100-56576) diluted 1:250, rabbit anti-Iba-1 antibody (Wako; 019-19741) diluted 1:250; rabbit anti- CD3 antibody (Sigma, SAB5500057) diluted 1:300, rabbit anti- CD20 (Invitrogen PA5-16701) diluted 1:750 followed by rabbit Mach-2 HRP-Polymer (BioCare; RHRP520L) for 30 minutes then counterstained with hematoxylin followed by bluing using 0.25% ammonia water. Labeling was performed on a Biocare IntelliPATH autostainer. All antibodies were incubated for 60 min at room temperature. Tissue pathology was assessed independently by two board-certified veterinary pathologists (AJM, RC).

RNAscope

RNAscope *in situ* hybridization was performed as previously described (Chandrashekar et al., 2020) using SARS-CoV2 anti-sense specific probe v-nCoV2019-S (ACD Cat. No. 848561) targeting the positive-sense viral RNA and DapB (ACD Cat.No 310043) as a negative control. In brief, after slides were deparaffinized in xylene and rehydrated through a series of graded ethanol to distilled water, retrieval was performed for 30 min in ACD P2 retrieval buffer (ACD Cat. No. 322000) at 95-98°C, followed by treatment with protease III (ACD Cat. No. 322337) diluted 1:10 in PBS for 20 min at 40°C. Slides were then incubated with 3% H2O2 in PBS for 10 minutes at room temperature. Slides were developed using the RNAscope® 2.5 HD Detection Reagents-RED (ACD Cat. No.322360).

QUANTIFICATION AND STATISTICAL ANALYSIS

Analysis of virologic and immunologic data was performed using GraphPad Prism 8.4.2 (GraphPad Software). Comparison of data between groups was performed using two-sided Mann-Whitney tests. Correlations were assessed by two-sided Spearman rank-correlation tests. P values of less than 0.05 were considered significant. Graphical Abstract was generated using BioRender.

Supplemental figures

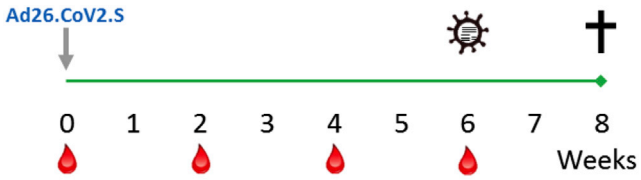

Group	Ad26.COV2.S	N
1	$1x10^{11}$ vp	5
2	$5x10^{10}$ vp	5
3	$1.125x10^{10}$ vp	5
4	$2x10^{9}$ vp	5
5	N/A	10

Figure S1. Study schema, related to Figure 1

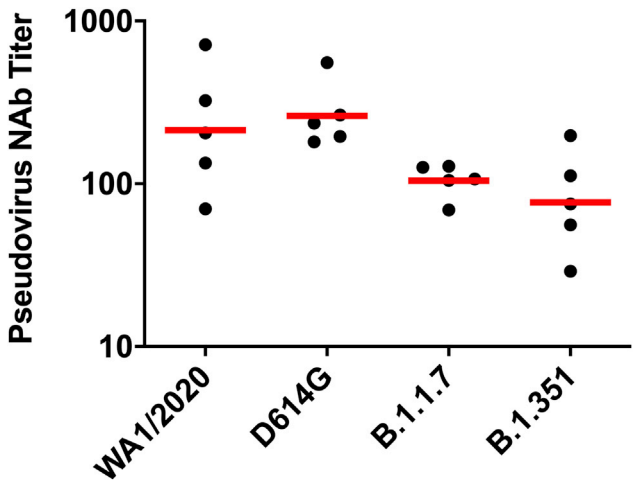

Figure S2. NAb responses against SARS-CoV-2 variants, related to Figure 1

Pseudovirus neutralizing antibody (NAb) assays elicited by $1.125x10^{10}$ Ad26.COV2.S (n = 5) against the WA1/2020, D614G, B.1.1.7, and B.1.351 SARS-CoV-2 variants. Horizontal bars reflect geometric mean responses.

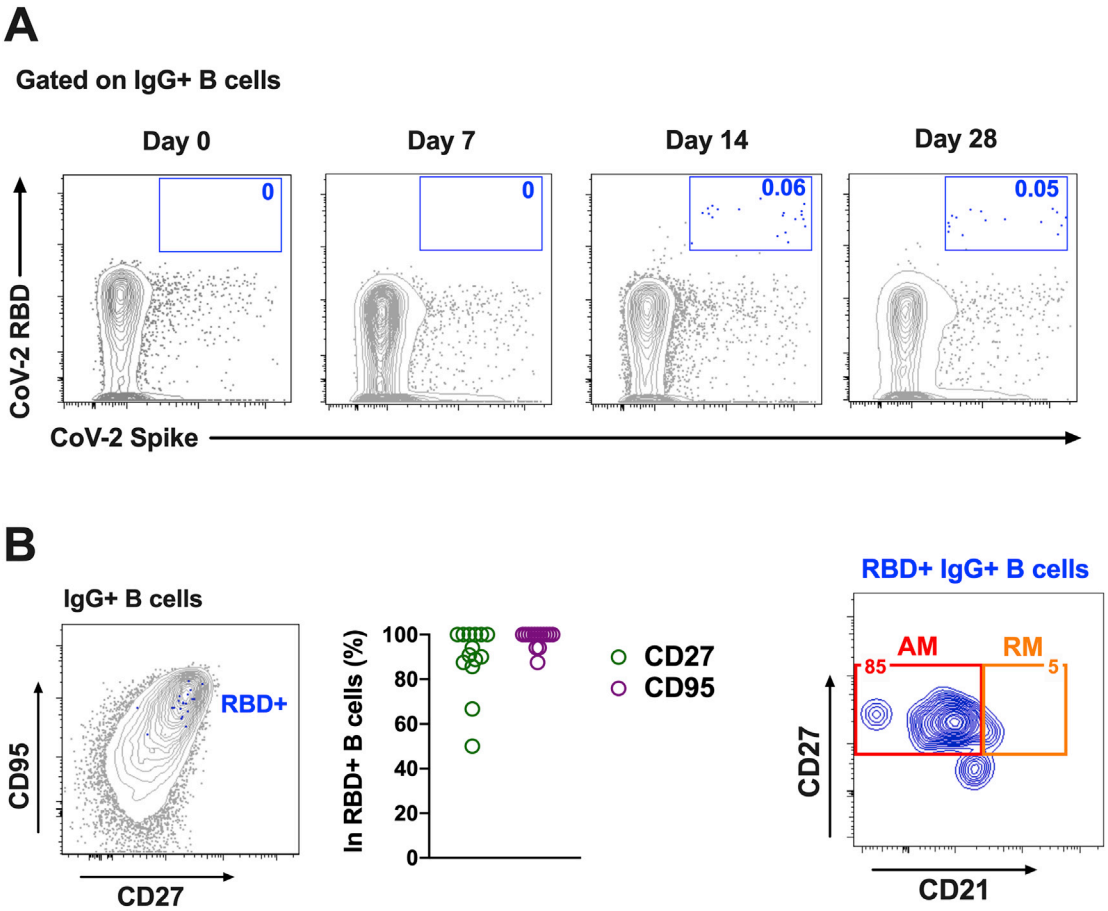

Figure S3. B cell responses in vaccinated rhesus macaques, related to Figure 3

Percentages of RBD-specific B cells in total IgG$^+$ B cell populations following Ad26.COV2.S immunization. (A) Representative flow cytometry of PBMCs from one monkey in the 1x10^{11} vp dose group at days 0, 7, 14, and 28 after vaccination, gated on class-switched IgG$^+$ B cells. (B) Expression level of CD27 and CD95 on RBD-specific B cells. (C) Flow cytometry showing activated memory (AM) and resting memory (RM) B cells, gated on RBD-specific IgG$^+$ B cells.

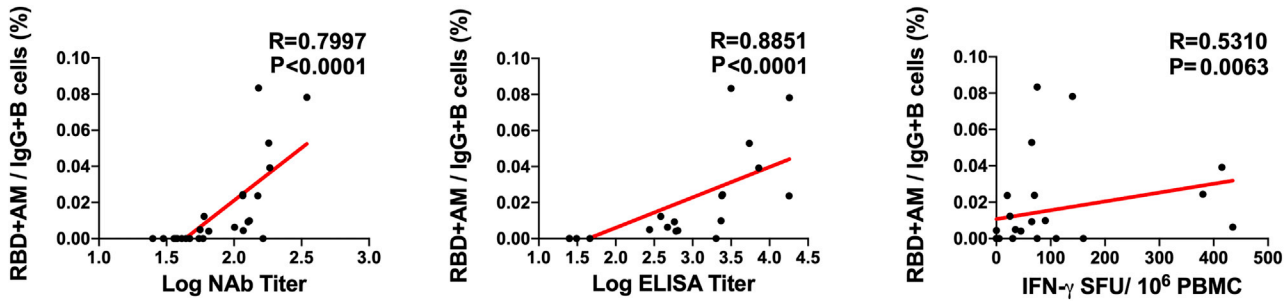

Figure S4. Correlations of B cell responses with antibody and T cell responses, related to Figure 3

Correlations of RBD-specific activated memory B cell frequencies with log NAb, log ELISA, and ELISpot responses in vaccinated rhesus macaques. Red lines reflect the best linear fit relationship between these variables. P and R values reflect two-sided Spearman rank-correlation tests. n = 25 biologically independent animals.

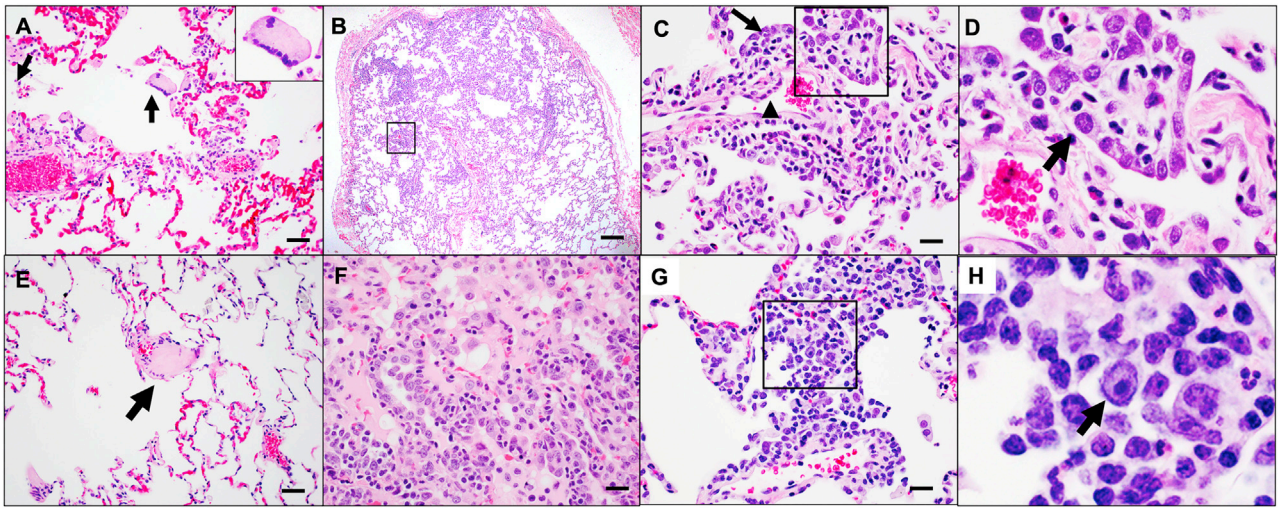

Figure S5. SARS-CoV-2-associated pathology in sham rhesus macaques following SARS-CoV-2 challenge, related to Figure 7

Focal to locally extensive SARS CoV-2 associated pathological lesions were observed in sham vaccinated monkeys 10 days following challenge. (A) Bronchoepithelial syncytia (arrow, inset) within alveolus; (B) Multifocal Type II pneumocyte hyperplasia; (C) Inset from (B) showing type II pneumocyte hyperplasia (arrow) and endothelial reactivity (arrowhead); (D) Inset from (C) showing hyperplastic pneumocytes (arrow) and occasional polymorphonuclear cells (PMNs); (E) thrombus (arrow); (F) focal edema and consolidation due to pneumocyte hyperplasia; (G) multifocal interstitial pneumonia; (H) Inset from (G) showing large reactive cells. Lesions shown are from 4 animals. Scale bars = 20 microns (G), 50 microns (A, C, E, F), 200 microns (B).

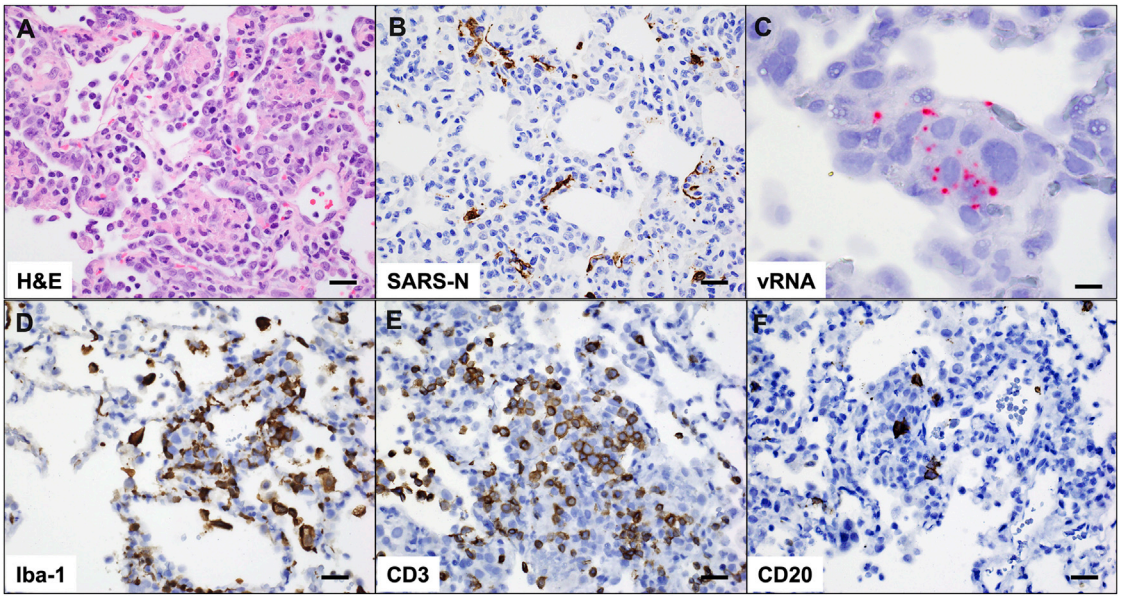

Figure S6. Pathology in sham-vaccinated animals corresponds to viral replication and inflammation following SARS-CoV-2 challenge, related to Figure 7

(A) H&E showing type II pneumocyte hyperplasia; (B) Immunohistochemistry for SARS nucleocapsid protein; (C) RNAscope *in situ* hybridization for viral RNA (vRNA) in hyperplastic pneumocytes. Immunohistochemistry for (D) Iba-1 (macrophages), (E) CD3 (T lymphocytes) and (F) CD20 (B lymphocytes) in regions of lung pathology. All images from one representative sham animal 10 days following SARS-CoV-2 challenge. Scale bars = 20 microns (A, B, D-F), 50 microns (C).